Vorticity Equation Terms for Extratropical Cyclones

RICHARD GROTJAHN*

National Center for Atmospheric Research,† Boulder, Colorado

(Manuscript received 16 May 1995, in final form 20 May 1996)

ABSTRACT

All terms of the frictionless, nonlinear, vorticity equation are examined. Traditional scale analysis provides one of several justifications for using the quasigeostrophic (QG) system of equations to model extratropical cyclones. Analysts of observations have long known that some of the other terms (non-QG) are individually comparable to terms kept in quasigeostrophy. While the non-QG terms are not small, they are assumed to have a large degree of cancellation and so are still neglected *in sum*. The distributions, magnitudes, and possible cancellations of vorticity equation terms are examined. Analyzed data composites for 15 cases of mature, developing, extratropical cyclones are used.

These results lead us to conclude that several commonly neglected terms are neither especially small nor do they cancel. The way each term contributes to the redistribution, advection, or amplification of vorticity is discussed. In sum, cyclone growth is greater at all levels, especially at low levels, in the full set of terms compared to the QG terms.

1. Introduction

The quasigeostrophic form of the equations has provided much theoretical insight into the dynamics of extratropical cyclones. Recently we have begun to study these frontal systems using models that have fewer approximations than the quasigeostrophic (QG) system. Models that have fewer approximations than the QG system but more approximations than the primitive equations (PE) are usually called "intermediate" models (e.g., McWilliams and Gent 1980). An example of an intermediate model is the "balance equations" (BE) system derived by Charney (1962). Before developing our theoretical, intermediate models, we decided to examine which terms had significant size in the observed (analyzed) atmospheric data. The purpose of the exercise was to provide us with a basis for including or excluding terms present in the primitive equations. We feel that our results are worth reporting for these reasons. First, we are not aware of a study that evaluates each term quantitatively using composites for numerous storms. Second, our results indicate that the tilting term, vertical advection of vorticity (ζ), and the relative vorticity times divergence term (ζD) are as large or larger than some QG terms at certain levels and locations. Third, we also find that they do not cancel to a high degree, contrary to statements by several previous authors. As for our original purpose in undertaking the study, we briefly comment on two approximations to the divergence term that have been employed in QG models.

The primitive equation vorticity equation is

$$\zeta_t = -\mathbf{V}_r\cdot\nabla\zeta - \mathbb{V}_d\cdot\nabla\zeta - \beta v_r - \beta v_d - fD - \zeta D - \omega\zeta_P + \mathbf{k}\cdot(\mathbf{V}_P\times\nabla\omega) \quad (1)$$

$$\mathrm{LC} = \mathrm{RA} + \mathrm{DA} + \mathrm{CR} + \mathrm{CD} + \mathrm{FD} + \mathrm{ZD} + \mathrm{VA} + \mathrm{TT},$$

where ζ is relative vorticity, $\mathbf{V}$ is horizontal vector velocity with r subscript for rotational component and d subscript for divergent component, v is meridional wind component, D is divergence, f is Coriolis parameter with meridional derivative β, ω is pressure velocity, and subscript P denotes pressure derivative.

In order to streamline the discussion that follows, we refer to specific terms by means of the labels under each term in (1). The QG system includes the following terms: LC (local change), RA (rotational wind advection), CR (Coriolis advection by rotational wind), and FD (Coriolis times divergence). The linear balance equations (LBE) form includes all QG terms plus CD (divergent wind advection of Coriolis). The balance equations (BE) form includes all the terms in (1); that is, the LBE terms plus DA (divergent wind advection), ZD (relative vorticity times divergence), VA (vertical advection), and TT (tilting term). In the figures that follow, we evaluate TT using only the rotational wind

---

* Permanent affiliation: Department of Land, Air, and Water Resources, University of California, Davis, Davis, California.

† The National Center for Atmospheric Research is sponsored by the National Science Foundation.

Corresponding author address: Dr. Richard Grotjahn, Atmospheric Science, University of California, Hoagland Hall, Davis, CA 95616-8627.

component (adding the divergent winds made little change).

The data we use are derived from data provided by NMC to NCAR and stored at T42 resolution. ("T42" refers to "triangular" truncation of spherical harmonics used to express each variable. The maximum wavenumber used is "42" in the zonal direction. Triangular truncation gives uniform resolution in both dimensions on a sphere.) All variables in the equations were calculated and interpolated onto a T106 grid using the NCAR CCM2 post processor (Buja 1994). The grid points used with T106 resolution are slightly more than 1° apart. Vertical interpolation was also performed onto a 10-level grid with nearly uniform vertical resolution in pressure. Derivatives in the vorticity equation terms were calculated using second-order finite differences on the high-resolution grid.

We selected 15 cases of storm development near the east coast of Asia drawn from four recent winter periods. While additional storms occured during the period, we selected these cases discussed here from a group of 28 that we had selected in a separate study of trough axis evolution. The other study used several criteria whose sole purpose was to identify those storms whose trough evolution could be unambigously tracked for five 12-h time periods. Satisfying those criteria was very laborious and is discussed in Grotjahn (1996). Our goal here was to select and isolate storms that have very similar gross structure in order to improve the consistency of the compositing procedure. Therefore, a subset of 15 cases was chosen having the greatest similarity in trough axis tilt. These 15 cases represented one-quarter to one-third of the total number of storms that occurred during the four winters. Data for the individual storms are listed in Table 1, including date, longitude and latitude of the surface cyclone center, and central pressure at sea level. It should be clear that in most cases the lows are strong, though in all cases the storms continued to amplify during the next 12 h.

In preparing the figures displayed, we composited the data from each case as follows. All terms were calculated for each case on the original (Gaussian) latitude–longitude grid for each case. The gridpoint values of the terms were shifted in the horizontal and averaged in time. The gridded values were shifted in longitude (and if needed, shifted a small amount in latitude) so as to place the origin in each case at the center of the low in 900-mb geopotential height.

The purpose of compositing the data is to find general results. We are not interested in, for example, explosive cyclogenesis, per se. Our cases include rapidly growing as well as slowly growing storms. The compositing process selects for those features that are common to the majority of storms while reducing the features that differ from case to case. We find considerable variation in the data fields from cases to case. Variation appears as small scale, "noisy" variations in fields that are magnified by taking derivatives and multiplications in some nonlinear vorticity equation (NLVE) terms. The composited fields (especially for vertical motion) are smooth. Variation also appears in the relative sizes and cancellations between terms in the NLVE. It is possible that the results for a particular case could create a misleading impression about how important a term actually is in the majority of other storms. Compositing is intended to avoid this problem.

TABLE 1. Cyclones used in this study.

Case number	Date	1000-mb center Latitude (°N)	1000-mb center Longitude (°E)	Central SLP (mb)
1	1200 UTC 11 December 1993	40	150	990
2	0000 UTC 12 January 1994	33	155	995
3	0000 UTC 15 January 1994	41	156	982
4	1200 UTC 29 January 1994	38	153	984
5	1200 UTC 9 February 1994	38	146	985
6	0000 UTC 7 January 1990	43	152	999
7	0000 UTC 17 February 1990	38	154	1006
8	0000 UTC 19 December 1990	38	153	987
9	0000 UTC 26 December 1990	40	135	997
10	1200 UTC 18 January 1991	41	154	993
11	0000 UTC 12 February 1991	43	157	990
12	1200 UTC 10 January 1992	41	167	979
13	1200 UTC 17 January 1992	42	138	1002
14	0000 UTC 1 February 1992	36	145	984
15	1200 UTC 24 February 1992	35	146	984

2. Composite evaluation of terms in the vorticity equation

a. Mass and wind fields

The mass and wind fields for the composites are shown in Fig. 1. The geopotential height shows a nearly constant rate of tilt with height. (When plotted using height as the vertical coordinate, not shown, the selected troughs are approximately straight lines.) The 200-mb trough is about 10° longitude upstream from the 900-mb trough. The lower-tropospheric center lies beneath the "inflection point" of the 200-mb pattern. A ridge lies ahead of the trough and has very little upstream tilt in the upper troposphere. One might speculate that the ridge's lack of tilt is consistent with diabatic, latent heat release in cloud masses associated with the warm front. Such an interpretation is consistent with the divergence field. At 500 mb there is a hint of horizontal tilt (southwest to northeast on the southern side of the trough). To the east and north, the ridge axis (and to a lesser degree the trough axis) has a northwest to southeast tilt. The horizontal tilts imply convergence of northward momentum flux above the surface low location; if so, one might speculate that the barotropic energy conversion may be negative. The rotational wind advection (RA) term includes the contributors to barotropic conversion in a kinetic energy

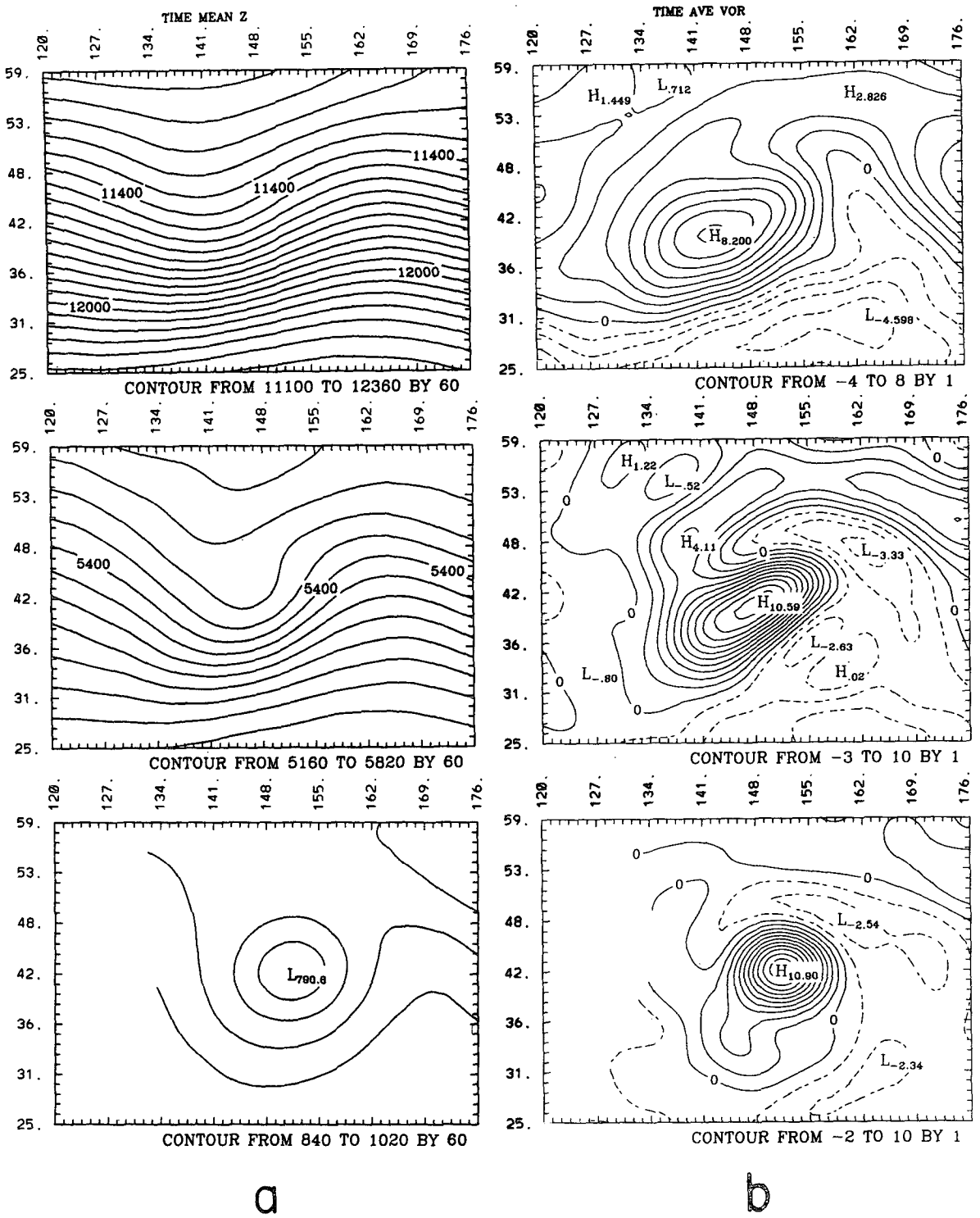

FIG. 1. (a) Geopotential height Z and (b) relative vorticity ζ at three levels: 200 (top), 500 (middle), and 900 mb (bottom). Values are time averages of 15 cases of mature but still growing extratropical cyclones. The data for each case were shifted to place the 900-mb Z minimum at the same grid point. The contour intervals are (a) 60 m and (b) 10^{-5} s^{-1}. The latitude and longitude ranges are averages for the 15 cases and primarily indicate the horizontal scale of the features.

equation. The tilt is more easily seen in the vorticity field.

Figure 1b shows relative vorticity at three levels. Since our study focuses on the nonlinear vorticity equation (NLVE), we shall use this figure to interpret NLVE terms. Interested readers may find it useful to prepare a transparency of Fig. 1 and to overlay it upon succeeding figures. The relative vorticity includes contributions from the trough (curvature) as well as the jet stream (shear vorticity). At upper levels, the positive shear vorticity on the north side of the jet (and negative values to the south) is readily seen. One should not emphasize how the relative vorticity maximum varies with height because the upper trough is not located at the same place in each case. While care was taken to match cases with nearly the same amount of upstream tilt, the difference between cases increases with height. The vorticity of the ridge ahead of the trough is weak.

In the next section, we discuss the contributions by each individual term in (1) to the total motion and shape change of the vorticity pattern. We may do this since the NLVE tendency LC is a linear sum of the terms in (1). Of course, one must keep in mind that the ultimate evolution of the pattern is the sum of all the terms.

b. Advection terms

The first term we consider has the largest peak values; RA is shown in Fig. 2a. Not surprisingly, much of this term reveals a translation of the vorticity field with the large-scale rotational wind. This is readily seen at 200 mb in the form of a dipole pattern. As can be seen from (1), the sign convention is that positive values of a NLVE term increase local vorticity, while negative values decrease the vorticity locally. Hence, a dipole having positive to the east and negative to the west implies motion from west to east. Figure 2a makes apparent that the motion has a slight northward component as well. The areal extent and magnitude of positive values ahead are both larger than the negative values behind the trough; one might conclude that RA contributes a net increase of relative vorticity at 200 mb ahead of the low. (A net increase would suggest an error in the calculation since this term cannot generate vorticity of the total field. However, one could identify barotropic conversion between eddy and mean flow from this term.) But part of the positive values seen in Fig. 2a ahead of the trough also include a separate dipole pattern for the weak ridge to the northeast. By mentally subtracting the ridge's dipole from the figure, one finds a roughly equal sized dipole about the trough with extrema located along an east–west line, implying primarily advection toward the east. At 500 mb, the shape of the low is being altered in an interesting way. In addition to motion toward the east northeast, the vorticity pattern is becoming more circular. At 900 mb the trough has a proportionally larger northward component than at the other two levels shown.

Peak values in Fig. 2a are 5×10^{-9} s^{-2}; individual cases often have peak values twice this size. However, some key features of the pattern in Fig. 2a are not unusual in the cases examined. In a dozen cases the pattern consists of a pair of maxima: one southeast and one northeast of the trough. In other cases, a simple east–west dipole prevails.

The advection by the divergent wind, term DA, is diagrammed in Fig. 2b. While DA varies in strength from case to case, it is one-fifth to one-twentieth the size of the RA term. Peak values in Fig. 1b are as much as 10^{-9} s^{-2}; on individual dates peak values are typically twice this size. While DA is routinely smaller than RA, DA is comparable to CR; in all but one case, peak values of DA exceed peak values of CR.

To understand DA (as well as several other terms) one must describe the divergence field D. By mentally removing f from Fig. 3a, one deduces the general pattern of the D field in our data. Low-level convergence is centered three to four tick marks due east of the 900-mb vorticity maximum in Fig. 1b. While DA contributes to the eastward propagation of the 900-mb trough, it is most evident that DA diminishes the intensity of the trough at this level (by reducing the area-averaged ζ). At 500 mb, DA is generally weaker than at the other levels since this level is closest to a level of approximate nondivergence (though Fig. 3a illustrates that D is not zero at this level). In the upper troposphere, D has divergence centered above the area of low-level convergence as one expects. At 200 mb, the divergence is centered at (155, 42) in the figures, with convergence centered 20° due west. These areas of convergence and divergence create most of the composite divergent wind at 200 mb. In addition, there are larger-scale divergent winds, primarily southeasterlies out of the Tropics occurring to the south and west of the trough. The larger-scale part of the divergent motion is consistent with climatology (e.g., Grotjahn 1993, Fig. 6.22, p. 278). The result of the two sources of divergent winds is a large decrease of vorticity on the southwest side of the trough plus northward motion on the west side of the vorticity maximum. To the southeast and immediately east of the vorticity maximum, ζ is decreasing. Farther northeast there is a slight indication of propagation to the northeast. The net effect of DA at 200 mb seems to be to weaken the trough on the southern side and possibly to spread the vorticity over a larger area on the northwest, north, and northeast sides.

Bosart and Lin (1984) present horizontal plots of several NLVE terms at three pressure levels for an explosively growing (Presidents' Day) storm. We may compare their Fig. 9 with the summation of our Figs. 2a and 2b. Their results at 300 mb have a similar dipole pattern with magnitude that is roughly seven times our values (not shown, but similar to 200-mb pattern shown). Their pattern at 900 mb has DA + RA (+ CR + CD) < 0 all around the low, with maximum value

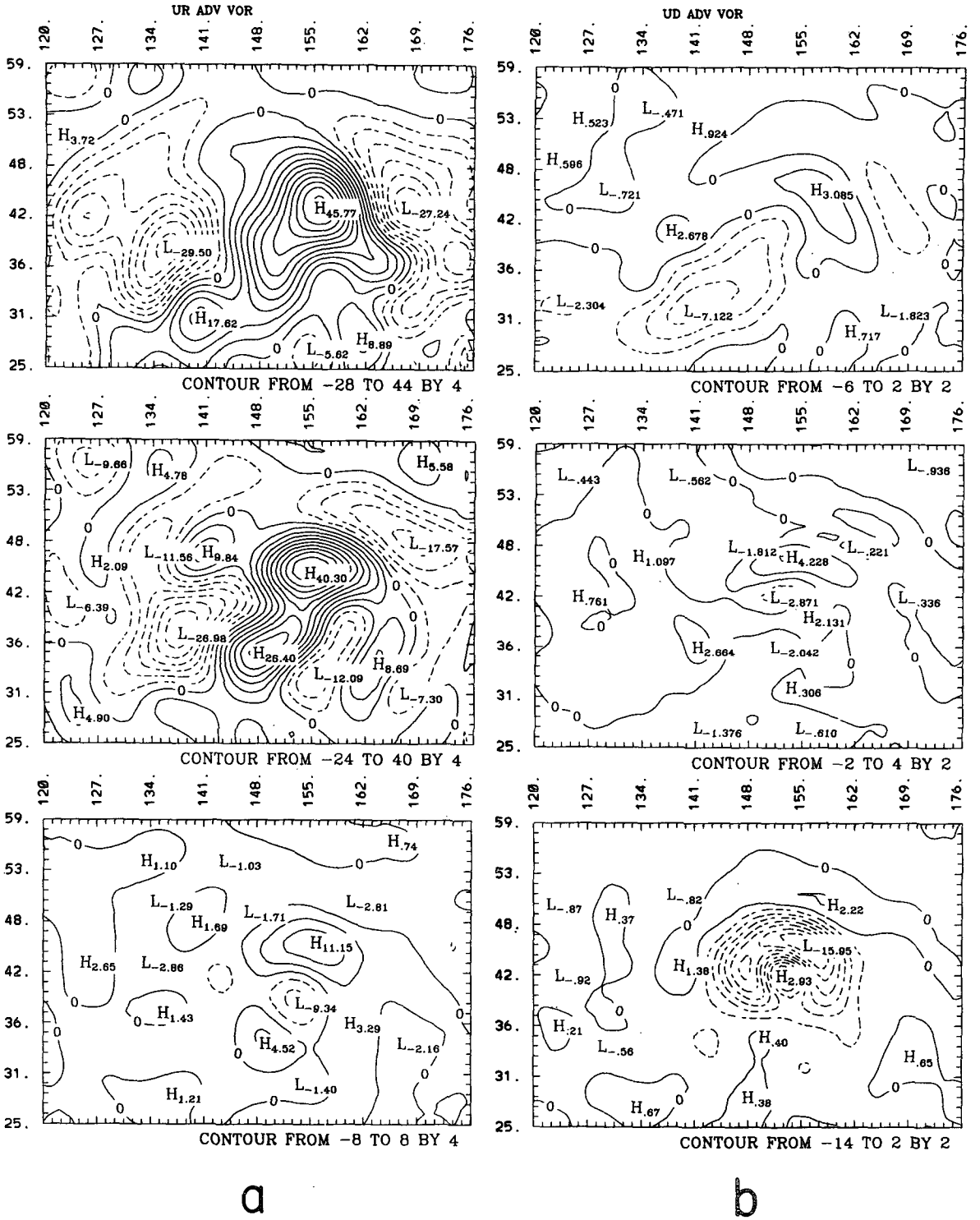

FIG. 2. Vorticity equation terms at three levels: 200 (top), 500 (middle), and 900 mb (bottom). Contour interval 2×10^{-10} s^{-2} is the same in Figs. 2–4. Terms (a) RA and (b) DA shifted in the horizontal in the same manner as used to construct Fig. 1 and then averaged over 15 cases.

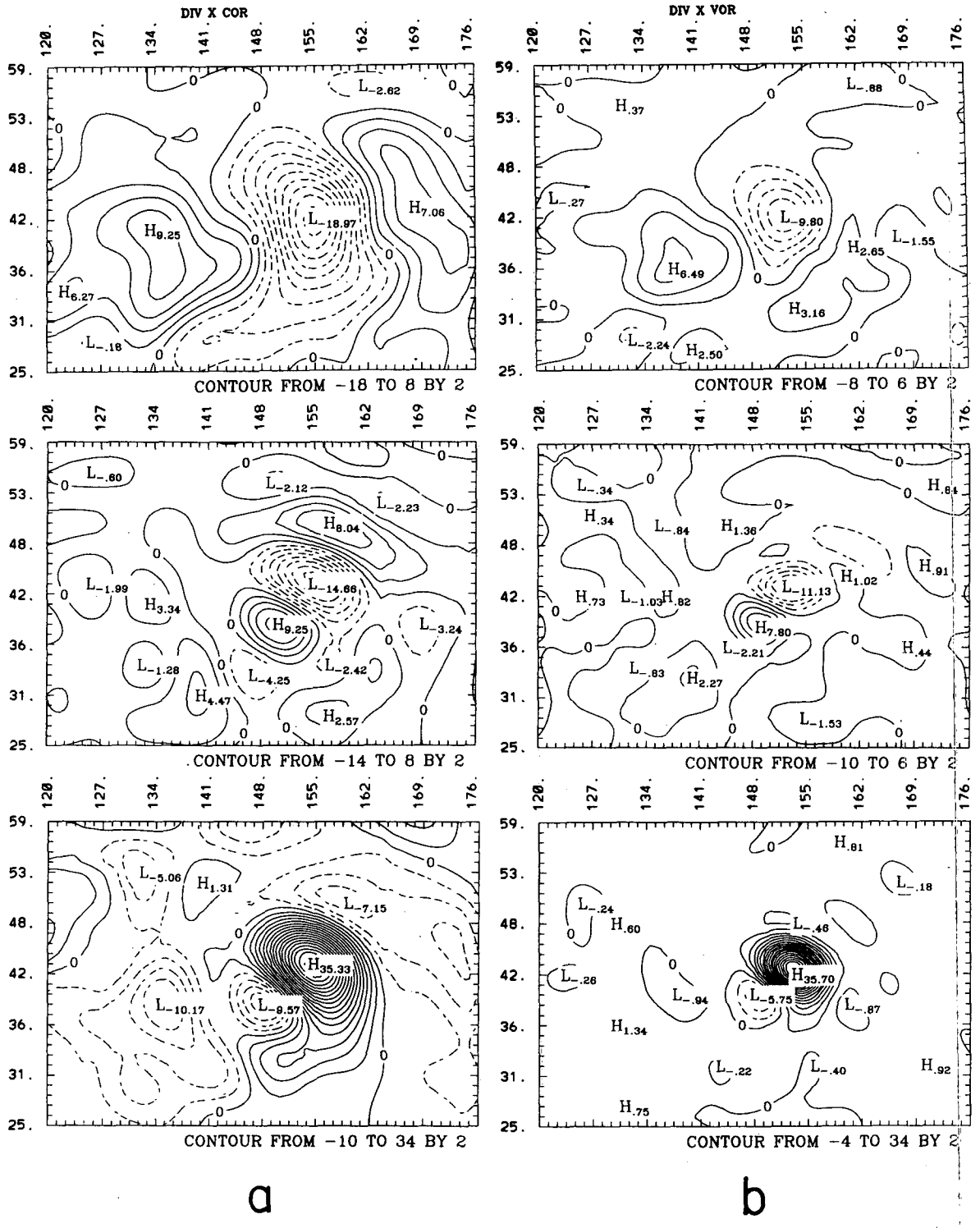

FIG. 3. Same as Fig. 2 except for (a) FD and (b) ZD terms.

roughly five times our results. (At this low level DA > RA in terms of peak values. Also, CR and CD are small compared to DA and RA.) Carlson's (1991) textbook includes a discussion of groups of NLVE terms estimated magnitudes for a particular cyclone over the eastern United States. Carlson has two estimates of

peak values for the horizontal advection of *absolute* vorticity by the *total* wind: 3 and 5 $\times$ 10^{-9} s^{-2}. His values are consistent with our estimate given that about 90% of the total horizontal advection is due to RA.

c. Coriolis terms

The variation of the Coriolis parameter contributes two terms in (1); namely CR and CD. These terms are small and have a very simple structure, so we shall describe, but not plot, CR and CD. Term CR has a dipole pattern reflecting the northward wind component east of the trough (negative CR) and the opposite west of the trough. As one expects, CR thus contributes to westward trough motion. Term CR has small variation with height, with a tendency for the negative region to have larger amplitude than the positive region. In about one-half of the cases, peak negative values are twice the peak positive values. Amplitudes are 3 $\times$ 10^{-10}–4 $\times$ 10^{-10} s^{-2}, less than one-tenth RA.

Because the large-scale flow has a meridional component that increases with height, the zero contour of CR lies west of the ζ maxima at 500 and 200 mb. This places the maximum values of ζ where CR < 0, implying some decrease to the peak ζ values. One should not expect the advection of planetary vorticity to cause any net change in *kinetic energy* from basic principles. Hence, the asymmetry of CR may be distorting the vorticity maximum into a more circular pattern and diminishing the central values, but one should not interpret such changes as weakening the extratropical cyclone. Term CD is routinely about one-tenth the size of CR, making CD by far the smallest of the terms considered here.

d. Divergence terms

The term FD is the term through which the QG system introduces baroclinic energy conversion. It is useful to consider the classic baroclinic instability description in addition to the distribution of D when examining this term. A classic result of QG theory is the baroclinically unstable normal mode as derived by Eady (1949), for example. The normal mode maintains a fixed structure (in particular, upstream tilt) in an environment with vertical shear. In a model like Eady's, this is accomplished by setting up a divergence field that reinforces the horizontal advection (term RA) below the steering level and opposes RA above the steering level. We can see that behavior in our results to the extent that FD has a dipole pattern that reverses with height. As for divergence, the Coriolis parameter has a simple enough variation across the domain that one can easily deduce the D fields from Fig. 3a. At 900 mb, the positive values ahead of the trough exceed the negative behind and the ζ maximum lies in a region of FD > 0. Therefore, FD increases the relative vorticity while propagating it toward the east and north.

At 500 mb, the dipole pattern may give an erroneous impression of transport toward the southwest. Comparison with Fig. 1b indicates that the relative vorticity pattern is being redistributed and the peak values are growing. The ζ pattern having the southwest–northeast orientation in Fig. 1b is stretched by FD into a more circular pattern through ζ growth on the southeast side (including the center of the low) and reduction of ζ at the northeast end. Propagation that may be occurring is comparatively weak.

At 200 mb, the pattern strongly shows the divergence above the warm front as well as convergence that is *centered* behind the trough. (Recall discussion of term DA.) Note that the divergent winds coming out of the Tropics help reinforce the convergence behind the trough. As at 500 mb, the dipole pattern is not centered about the trough but is located such that the trough center lies in a region of positive FD. Term FD is increasing the peak ζ values at this level as well. The FD dipole pattern is larger and more symmetric about the trough than it was at 500 mb, so FD contributes stronger propagation than at other levels shown. The propagation is obviously toward the west. Clearly, the main features of the FD pattern are very consistent with the normal-mode model of cyclogenesis: growth at all levels and maintenance of the tilt against the shear.

One would expect the FD term to be a sizable term if one believes that baroclinic instability plays a sizable role in extratropical cyclone dynamics. As stated earlier, FD is a term kept in QG models. Here the peak values are 2 $\times$ 10^{-9}–3 $\times$ 10^{-9} s^{-2}. The peak values of FD are about one-half the RA values, but at specific (lower) levels FD exceeds RA. Peak FD values are between two and three times the peak values in the divergent wind advection term, DA in every case studied. The impact of the FD term is likely to be a bit stronger than this comparison of the peak values implies since FD typically has significant values over a larger domain than DA.

The divergence term arising from relative vorticity, ZD, is shown in Fig. 3b. In the QG system of equations this ZD is ignored. It is obvious from the figure that this term is comparable to FD for the well-developed (but still growing) cyclones composited here. In comparing Figs. 3a and 3b, it is obvious that ZD has a very similar pattern as FD, just smaller amplitude. The large values of ZD at 900 mb are partly a testimony to the large amplitude of the low, however, so the ratio between ZD and FD would be reduced if the low was weaker. Neglecting meridional propagation, f would not change over a period of cyclone development, but the ratio of ζ relative to f would be smaller at earlier stages. The ζ/f ratio could be much less at low levels, but the change would not be as dramatic in the upper troposphere due to the jet stream vorticity. The sign of ZD is similar to FD because low-level convergence occurs near the low where $\zeta > 0$; at upper levels, the divergence occurs where the *tendency* of ζ is negative,

but still where $\zeta > 0$ due to the shear vorticity of the jet stream. Term ZD is comparable to FD in most individual cases studied here. More is said about the possible cancellation of this term with others in section 4.

We may compare the combination of FD + ZD in Fig. 3 with results by Bosart and Lin (1984) for the Presidents' Day storm. At 300 mb, they have a dipole structure similar to our results (not shown, but similar to 200 mb) except that the pattern is shifted west relative to the trough axis, compared to how our dipole straddles the trough. Their peak values are about five times the peak values we find. At 900 mb, they have a primary maximum in FD + ZD as do we, though in their case it is centered north and slightly west of the trough center (ours is east). Their peak values are about twice ours. So while the patterns have much similarity, the relative sizes are a bit different between our composite and their case. Carlson (1991) has two estimates: 1.4×10^{-9} and 1.5×10^{-9} s^{-2}, which are roughly one-half of the magnitude of our peak estimates.

e. Vertical motion terms

The vertical advection of relative vorticity is term VA in (1), and Fig. 4a shows the composite distribution for the 15 cases studied. Larger values of VA occur in the midtroposphere, partly reflecting relative extrema in ω there. At 500 mb, the central, negative values of VA occur where downward motion aligns with a small region where ζ increases with P. The main contribution comes from the positive areas of VA. Ahead of the trough upward motion and increasing ζ with P combine; behind the trough downward motion with decreasing ζ combine to give VA > 0 maxima. The net effect of this term is to increase vorticity ahead of the trough with a slight decrease near the center and further increase behind at 500 mb. So VA is expanding the region of positive ζ at this level. At 200 mb there is some indication of ζ propagation to the northeast along with a net increase in ζ. So VA appears to amplify, expand, and move east the upper-level trough. In the lower atmosphere, there is some decrease of ζ at and ahead of the trough due to the combination of rising motion with vorticity that decreases with P.

To understand better the distribution of VA, Fig. 5 relates the zonal and vertical components of the divergent circulation to the trough and ridge axes. The axis of maximum relative vorticity (Figs. 1 and 5) lies east of the trough axis in the middle and upper troposphere. In addition, two relative maxima occur along this axis (dotted line in Fig. 5): one at 400 mb and the other (weaker) at 800 mb. The divergent circulation in the zonal plane consists of strong rising motion that is centered between the trough and ridge axes at most levels. The maximum downward motion lies well behind the trough in geopotential height Z; a secondary maximum downward motion lies closer west of the trough. The divergent wind u_d also has a tendency for a double maximum in the composite data with relative maxima close to and farther behind the trough. Most features seen in Fig. 4a can easily be deduced from information in Fig. 5. For example, the negative VA at 900 mb results from upward motion where the axis of ζ is more vertical than above (while also approaching a relative maximum at 800 mb).

Here VA has largest values in the composite data at 600 mb. In Fig. 4a, the peak value is -7×10^{-10} s^{-2}. Term VA has much variation between individual cases; in nine of the cases the peak positive values greatly exceed the negative values at 500 mb, while in most remaining cases the magnitudes are similar. In a few cases peak positive values of VA at 500 mb are as much as one-third of peak values of RA; typically, peak VA values are one-sixth of peak RA values.

One might view the DA and VA terms as redistributing ζ in the following manner. At low levels, DA mainly reduces ζ about the low and moves it slightly ahead, much of VA is canceled by DA at this level. In midlevels (around 500 mb), VA is stronger than DA and is distributed so as to increase the areal extent of the larger positive values of ζ. In the upper-troposphere DA is tending to spread apart the trough and ridge (moving the ridge north and pushing the trough west). Hence, the divergent advection terms DA and VA appear to oppose the tilting into the vertical of the trough axis.

The tilting term (TT, Fig. 4b) is also largest in the midtroposphere in large part because ω has larger amplitude there. In the composite data TT has negative values along two axes: one region lies north and west of the surface warm front, while the other lies along most of the cold front. Running along an east–west line drawn above the surface low center are positive values. The vertical shear in the meridional and zonal components of wind are both negative (southerly and westerly flow increase with height) over most of the area where TT is large in Fig. 4b (at 500 mb). Term TT has four extrema due to the "comma-shaped" distribution of rising motion ahead and north of the trough, along with two maxima in downward motion located to the west. The double maximum in ω was mentioned in discussing Fig. 5. A schematic diagram of the horizontal distribution of vertical motion at 500 mb is presented in Fig. 6. The figure was produced by tracing key features from contour plots of composites fields. Figure 6 includes a bold "L" to mark the 900-mb low center, a dashed contour to illustrate the 500-mb Z ridge and trough, and the four regions where extreme values of TT occur.

The negative values ahead of the warm front (area W in Fig. 6) neatly match the minimum in ζ (Fig. 1b). Rotating the horizontal vorticity of the vertical shear of the zonal wind into the vertical component (ζ) reduces ζ because the upward motion decreases (then becomes downward) as one proceeds northward. Along the cold

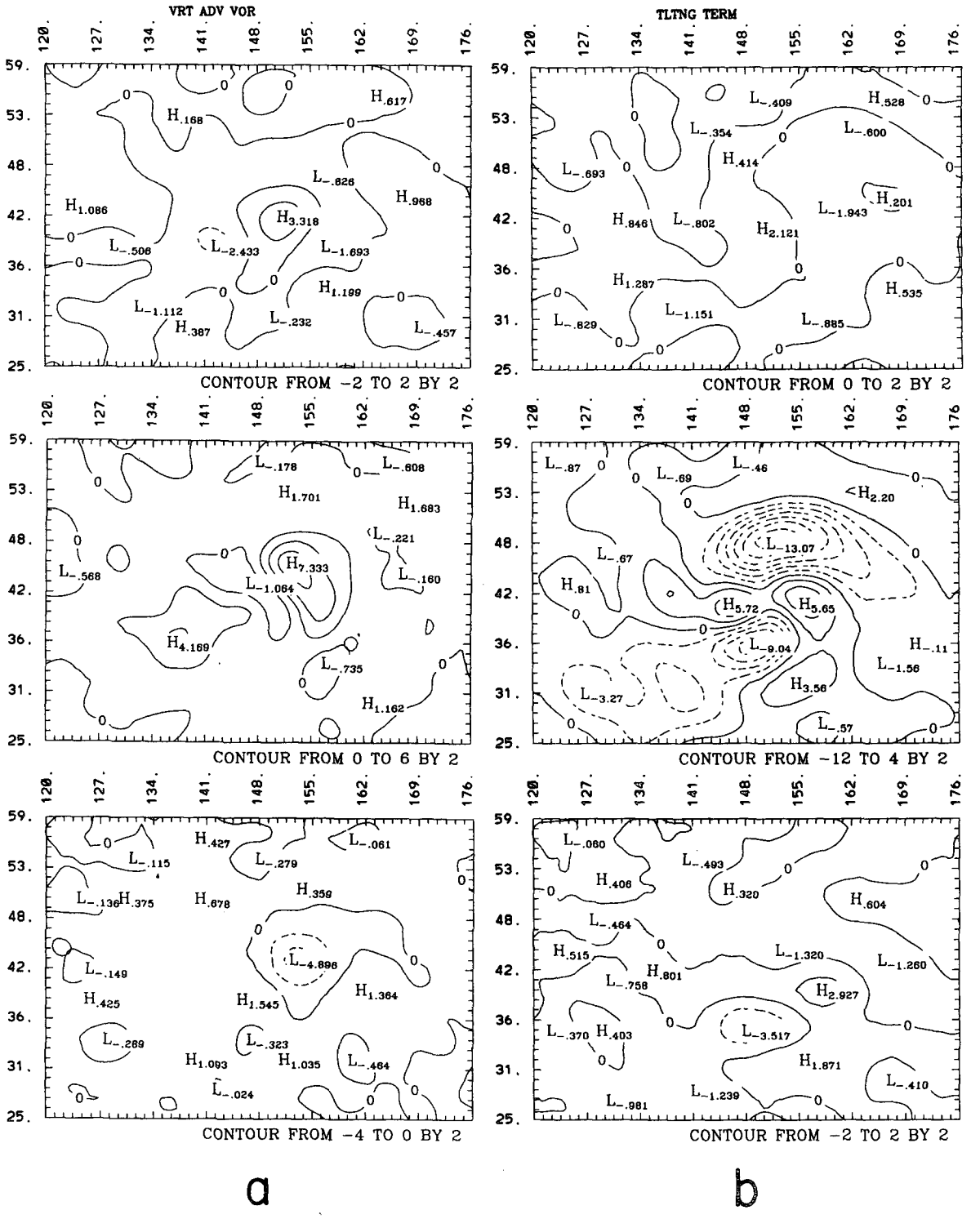

FIG. 4. Same as Fig. 2 except for (a) VA and (b) TT terms.

front (region C in Fig. 6) $\mathbf{V}_p$ and $\nabla\omega$ are both positive making TT < 0. The horizontal vorticity of the zonal wind shear and the meridional wind shear both are rotated into the vertical to subtract positive vorticity from the vertical component ζ. East of the surface low the upward motion increases with latitude so TT is posi-

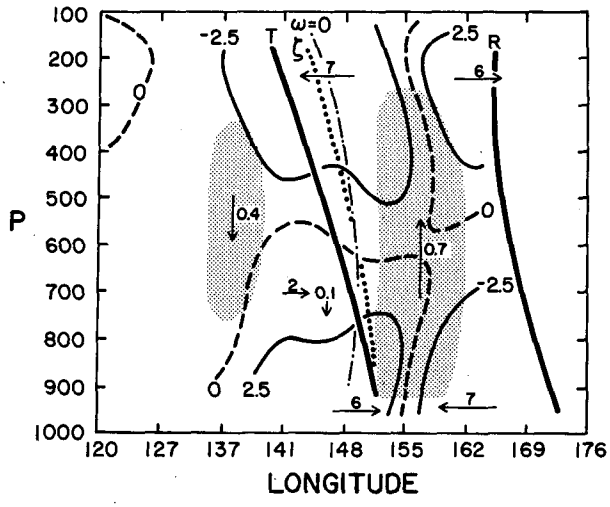

FIG. 5. Schematic zonal cross section transcribed from analyses of Z (T for trough, R for ridge axes), ω (shaded areas for ω magnitude greater than 0.25 Pa s^{-1}, and dot–dashed line for $\omega = 0$), and zonal component of divergent wind, u_d (solid contours for ± 2.5 m s^{-1}, dashed contour for $u_d = 0$). The axis of minimum relative vorticity lies atop the ridge (R) line. The maximum relative vorticity is shown with a dotted line that lies at or east of the trough axis. Arrows are centered at relative extrema with numeric labels of the local speed. The cross section follows 41°N and is intended to assist interpretation of Fig. 4a.

tive. West of the surface low the upward motion increases with latitude (note the secondary maximum in Fig. 6 between A and C) and also has a small region where downward motion increases with longitude east. Above the surface low the two parts of TT nearly cancel.

In the net, TT is tending to amplify the peak values of the trough in the midtroposphere and possibly to elongate the trough in the east–west direction. In the meridional direction, TT is tending to reduce the length scale of the trough. Peak values of TT reach 1.3 $\times 10^{-9}$ s^{-2} at 500 mb (higher at 600 mb). As with VA, this term has much variation between cases. Most cases have a negative area somewhere near where the warm front would be expected (area W). An area behind the trough, sometimes farther west than area A, is also fairly common. Areas of alternating positive and negative value (like area B with a smaller area C) occur less often and are located less consistently in the cases. Peak values of TT are often similar to peak values for ZD and greater than or comparable to peak values in VA. Hence, while peak values of DA, ZD, VA, and TT are all smaller than RA, they are often not an order of magnitude smaller. Peak values of DA and ZD (near the top and bottom) and VA and TT (in the middle troposphere) are all comparable to peak values of FD (near the top and bottom). All these terms are usually greater than peak values of CR.

Bosart and Lin (1984) do not present contour plots of the vertical motion terms. However, they do present volume averages in several layers at different times. Not surprisingly, VA and TT are larger in the midtropospheric layer. Interestingly, they are the largest terms early in the cyclone development. Carlson's estimate of VA is 5 $\times 10^{-10}$ s^{-2}, which agrees well with the values found here. Carlson's estimates of TT are 7 $\times 10^{-10}$ and 10 $\times 10^{-10}$ s^{-2}, which are one-half to two-thirds of the peak values found here.

3. Some thoughts on scale analysis

a. General considerations

The purpose of scale analysis is to estimate the magnitudes of terms in an equation so that one might isolate the most important terms. The results might be used to develop a good approximation to the equation or to identify which physical processes are most important.

A scale analysis is not simply substituting dimensional scales for parts of terms. A well-known example is the proper scaling of the vertical velocity. Large-scale vertical velocity W does not simply relate to horizontal velocity V by means of the spatial aspect ratio (H/L; where H is vertical and L is horizontal length scale) due to the static stability of the large-scale flow.

When scaling derivatives, one replaces the differential operator with the range of the quantity differentiated divided by the distance over which that range occurs. For a sinusoidal variation, the spatial derivative could be estimated as the amplitude of the wave divided by the *quarter* wavelength. Since the actual peak values of the derivative equal 2π times the amplitude divided by the wavelength, the estimated scale approximates well the derivative averaged in the vicinity of the peak values.

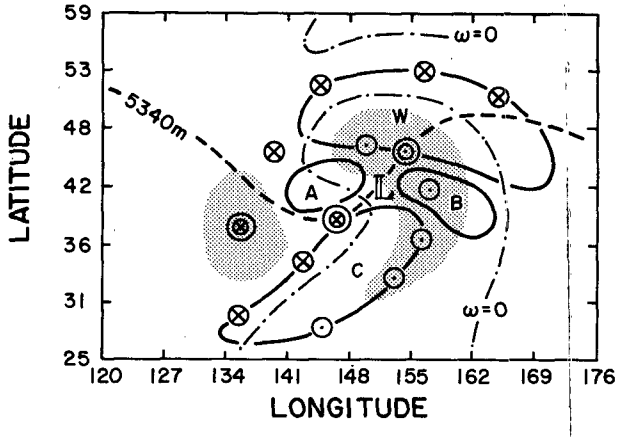

FIG. 6. Schematic diagram of the distribution of vertical motions at 500 mb relative to the trough at 900 mb (block "L" marks the center) and the 500-mb trough and ridge (dashed contour of 5340-m Z plotted). Shaded areas are as in Fig. 5: vertical motion magnitude exceeding 0.25 Pa s^{-1}; dot–dashed line is the contour where $\omega = 0$. Circles with a dot indicate upward motion; circles containing an "X" indicate downward motion; a double circle is drawn where a relative maximum or minimum occurs in ω.

The discussion above helps explain why the results presented here differ from some published works but not others.

First, it is commonplace to choose the nearest power of 10 for a scale (e.g., $V = 10\ \mathrm{m\ s^{-1}}$). While this rounding off may be reasonable for individual scales, it is possible for the rounding off error to accumulate when several scales are multiplied in order to estimate one term. A trivial illustration is to consider two scales A and B. Observations may indicate that $A = B = 1/3$. If A and B are each scaled as order 0.1, then one might conclude that the product AB is of order 0.01. This estimate would be off by an order of magnitude.

Using powers of 10 to scale the tilting term (in pressure coordinates) can be misleading. Assuming scales: $P = 10^5$ Pa, $L = 10^6$ m, $V = 10\ \mathrm{m\ s^{-1}}$, and $W = 10^{-1}\ \mathrm{Pa\ s^{-1}}$ gives an estimate of TT $= 10^{-11}\ \mathrm{s^{-2}}$. This estimate implies that TT is two orders of magnitude smaller than the rotational advection terms. However, the scaling is quite different if we use observed values. Using peak values of omega gives an estimate of $W = 0.5\ \mathrm{Pa\ s^{-1}}$. The vertical velocities are somewhat concentrated near the frontal zones (even for the large-scale data here), hence the length scale for horizontal derivatives of omega is less than the L that is apropos for other fields (like geopotential or possibly horizontal velocity components). A reasonable value for the tilting term is $L = 2.5 \times 10^5$ m. The vertical shear of the Asian subtropical jet is much larger than our "traditional" estimate. Hence, over the lowest 500 mb, the wind may easily increase by $25\ \mathrm{m\ s^{-1}}$. Using these scales, TT has magnitude $10^{-9}\ \mathrm{s^{-2}}$. This estimate is 100 times larger and suggests that the tilting term is comparable with the quasigeostrophic terms. This result compares favorably with estimates by others (e.g., $7 \times 10^{-10}\ \mathrm{s^{-2}}$ in Carlson 1991) and with results presented in section 2e. Holton's textbook (1992) assumes powers of 10 in such a combination that TT and VA are both an order of magnitude smaller than FD. On that basis he neglects these terms. Such a scaling is suitable for a text and for large-scale flows in general, but it is not necessarily suitable for the specific situation of extratropical cyclones developing along a strong jet.

A second subtlety is to sample all portions of the domain containing the phenomenon of interest. Terms have varying importance in different regions. Terms VA and TT are small near the bottom of the troposphere but both are much larger in midlevels. (The variation reflects the amplitude profile of vertical velocity.) Petterssen (1956, p. 323) states that "computations show that [VA] contributes but little to the vorticity production." He appears to be discussing vorticity production at the surface. It is possible he was simply referring to the amplitude of VA at low levels (which would be consistent with results shown here). Palmén and Newton (1969, p. 251) evaluate TT and find it large in the midtroposphere in a cross section through a front. Carlson (1991, p. 56) estimates VA in the midtroposphere to be roughly one-third of the size of FD. Carlson (1991, p. 62) finds TT to be a bit larger than VA and comments that TT "may be important and even dominate at upper levels in the vicinity of fronts or jet streaks . . . ." Reed and Sanders (1953) find that TT exerts "the controlling influence on vorticity changes in the middle troposphere" in a study of frontogenesis.

The interest here is upon terms having an impact upon the synoptic-scale weather system. One might argue that TT is large for frontogenesis (say) but that it is a mesoscale, not synoptic-scale, phenomenon. In Holton's textbook (1992, p. 108) he concedes that TT and VA become important near fronts. While the across-front length scale of large values of TT is smaller than the length scale of ϕ (by one-third, say), one must recognize that the large values of TT extend for a much longer distance in the alongfront dimension. This example illustrates a third subtlety of scale analysis: that magnitude and areal extent both play a role in determining the scales used and significance of a term.

A fourth subtlety is that terms that appear large may have a large degree of cancellation. The classic example is the two parts of the divergence of the horizontal wind. Reed and Sanders (1953) state: "the [tilting] terms have received little attention in problems relating to vorticity change. The results presented here suggest that they may well be deserving of more consideration. . . ." Why then has it been so common to neglect the tilting term? When a reason is given, an author neglects terms TT, VA, and ZD because the terms are believed to have no net impact upon the *large-scale* development process. We now examine this belief.

b. *Do higher-order terms cancel?*

Sutcliffe (1947, p. 374) recognizes that TT may be large but makes an argument claiming that the ZD and TT terms have a large amount of cancellation. We can easily test this idea by comparing the distributions of these two quantities in Figs. 3b and 4b. Based upon the distribution of D, ζ, and ω, the argument is unlikely to hold at individual levels since ZD is largest at top and bottom, while TT is largest in the midtroposphere and small at top and bottom. Having said this, one can compare the locations and magnitudes of the extrema in both fields and thereby make a rough estimate. It seems clear from the patterns at all three levels that the two fields have about as much reinforcement as they do cancellation. Based on this evidence, we are inclined to doubt whether ZD and TT cancel. However, we have looked further and summed the two terms for individual cases. In 6 of our 15 cases, much of the ZD contribution is canceled by TT; in most of these 6 cases, we also find that TT is largely reduced by the summation. In most of the remaining cases, about as much

reinforcement as cancellation occurs, as the composite data shows. So it is at least possible that Sutcliffe's physical (and mathematical) argument was reinforced by the specific data available to him. It is also possible that approximate techniques for estimating D may play a role in concluding that TT is canceled by other terms; this possibility is reexamined in section 3c.

Arnason and Carstensen (1959) calculate TT and VA at 500 mb for the Northern Hemisphere and show how the terms alter ζ over four forecast periods. They find nearly exact cancellation between them when they are summed. Bosart and Lin (1984) remark that such a cancellation tended to occur in an earlier study of a tropical cyclone, but such cancellation was *not* the case for the Presidents' Day cyclone they studied.

Dutton (1986, p. 343) presents a scale analysis that implies that TT may be comparable to FD. Later however (p. 360) he states that TT "is often omitted, on the grounds that tilting terms tend to cancel the vertical advection of vorticity. This assumption is not always true, however." And later (p. 362): "observational evidence suggests that the [VA and TT] terms tend to cancel each other, and that their sum is smaller than the other terms of the vorticity equation." These statements provide another test of our data. As with Sutcliffe's assertion, we find mixed evidence for cancellation between these terms. At least in this instance, TT and VA have similar amplitude variation with height. However, inspection of Figs. 4a and 4b implies that there is roughly as much reinforcement as there is cancellation between these two terms. We also examined the sum of VA and TT for individual cases (as with VA, the TT pattern for individual cases is often more complex than Fig. 4b: more extrema having less smooth shapes appear, typically). In 3 of the 15 cases we find a lot of cancellation between VA and TT; two of these three are cases where ZD and TT also have a large degree of cancellation. Even in cases of significant cancellation, we still see continued reinforcement between VA and TT in the vicinity of the upper-level trough.

Other reports allow comparison of the VA and TT terms. Krishnamurti (1968) compares terms in the "ω" equation, including terms that arise from VA and TT. In considering the development of a cyclone over North America, he states that the contributions by these two terms to the vertical motion "have a tendency to cancel each other." Since VA and TT have similar vertical structure (and the same linear operator applies to VA and TT in the ω equation), it is reasonable to conclude that VA and TT would largely cancel in his case. In contrast, Whitaker et al. (1988) find much reinforcement between VA and TT in the Presidents' Day cyclone. They present cross sections of six terms in the NLVE; each cross section is oriented along an axis of maximum 850-mb ζ, which roughly follows the cold front. In their cross sections, VA and TT are large and have a very high degree of reinforcement. These studies illustrate how difficult it is to generalize from a single case.

One may wonder about the sum of all three terms: ZD + VA + TT. In one additional case the amount of reinforcement and cancellation is such that the combination of all three terms creates a lot of cancellation. So, in 7 of 15 cases, there is more cancellation than reinforcement between TT and some other term(s). One can verify this by overlaying Figs. 3b, 4a, and 4b while keeping in mind the sensitivity of ZD to storm amplitude mentioned earlier. Since terms like TT are comparable to FD, we conclude that the degree of cancellation is probably not sufficient to justify neglecting the higher-order terms (ZD, VA, and TT) while retaining FD. In other words, the sum of ZD, VA, and TT may have comparable effect as term FD.

c. *An indirect effect*

The QG approximation is more than simply neglecting certain terms in the NLVE. The value of divergence D differs, making the term FD different in the QG and BE (say) systems of equations. This difference is now briefly described.

When assessing the proposed cancellation between terms like ZD and TT, one is keenly aware that D and ω are not directly measured. We, as well as previous authors, must estimate divergent circulations by some means. We have used values calculated by the CCM2 postprocessor that are derived from a primitive equations (PE) model. We make the assumption that the D and ω obtained in this way are sufficiently accurate to represent the large-scale flow. Not all scale analyses have had the luxury of archived data from a PE model. Rather than attempting to examine if our estimates of divergence differ from others, we focus on how expressions in some simple QG theoretical models give varying estimates for divergence.

In designing simple QG models, it is commonplace to express the FD term using the streamfunction (or geopotential) so as to obtain a potential vorticity equation having just one prognostic variable. Depending on the approximation used, D may be proportional to the two-dimensional total derivative of the second vertical derivative of streamfunction [ψ; e.g., the form used by Eady (1949)]. Relaxing some of the approximations, one can express D as the two-dimensional total derivative of a function of geopotential ϕ and pressure (e.g., the form used in Grotjahn and Wang 1990). In order to retrieve one equation with one unknown, we may use one of several balance relations between ψ and ϕ.

For a QG formulation, one would use a linear balance relation and could include variation in f. Here we improve the approximation by using *observed* geopotential; one may view this as including a higher-order balance relation than used by the ψ form. Solving for D requires evaluating a time derivative. We used successive time samples, but unfortunately the interval of 12 h is very large.

It is not surprising that the ψ form does worst at all levels. The ϕ form does a better job of picking up the maxima at upper levels than at the lowest level. The PE form has convergence at the center of the 900-mb trough; the ϕ form has convergence centered just northeast of this trough. The ψ form has *divergence* at the trough center. At the lowest level one would expect some portion of the divergence to respond to boundary layer friction. We have not included any diabatic process. Friction might be included by incorporating, say, Ekman pumping. The ϕ form is most similar to the QG formulation used by Simmons and Hoskins (1976) in their comparison of linear QG and PE simulations of idealized cyclones. Simmons and Hoskins remark that "the quasi-geostrophic divergence is remarkably close to the primitive equation value over the whole range of" cases they study.

We compared how all three of these calculations of D altered the possible cancellation between ZD and TT for the one case studied here. The results did not display any consistent pattern. A combination that had more cancellation than others at one level would have less than the others at another level.

4. Summary and discussion

We have shown composites of the gridpoint values of eight terms in the vorticity equation for 15 cases. The cases were selected for actively growing, large-amplitude (i.e., mature) extratropical cyclones that had similar upstream tilt (uniform with height) and similar geographic location. We made comparisons with observational studies in the discussions of each term and found results that were generally similar. Below are specific results for this study.

The rotational wind advection is the largest term and it primarily moves the trough eastward and slightly northward. The motion is greater at upper levels in response to the vertical shear of the mean wind. The divergence terms FD and ZD oppose the *differential* propagation by the RA term. Terms FD and ZD encourage moving the lower trough ahead while holding back the upper part of the trough. The opposition between FD and RA is consistent with classic theoretical models. The planetary vorticity terms (CR and CD) are small, with the divergent advection of f (term CD) being the smallest of the terms by far. Peak values of remaining terms VA and TT are comparable to peak values of FD, though VA and TT have larger values over a smaller domain than FD.

The higher-order terms alter the development and propagation of the cyclone in somewhat different ways for different cases. Collectively, these terms alter the shape as well as the amplitude and motion of the trough. The distribution of pressure velocity ω largely follows a classic pattern, and from that pattern one may deduce the qualitative distribution of TT accurately. The distribution of VA is less easily deduced from the classic model in part because the upper-level ridge does not overlie the surface low. Terms VA and TT appear to increase the trough amplitude in midlevels, but one may be expanding the area of large vorticity while the other may be shrinking it.

The total effect of the terms on the right-hand side of (1) may be summed. This sum provides our estimate of LC and is presented in Fig. 7b. Alternatively, one could estimate LC independently by means of a finite difference in time of the vorticity field; that estimate (not shown) is not useful due to the large time interval between data. During the 24 h of a centered-in-time difference, the vorticity center associated with the trough in most cases moves quite a distance (another property of examining the region of a strong jet). Because of this movement, the peak values in LC at a given point along the storm track are much larger than the 24-h time average value of LC at that point. (When we examined a few cases in detail, not shown, we found differences in the peak values of LC of a factor of 3.) The problem with a large finite difference in time can be visualized in this way: the maximum and minimum LC found this way are centered where the vorticity maximum is at the later and earlier times, respectively. These locations do not correspond to locations of the strongest gradients in ζ at the intermediate time.

Figure 7 shows two estimates of LC. The left column estimates LC using the terms kept in the QG system. While these terms are kept by the QG system, their evaluation may differ from a QG model. For example, we used full divergence, not the QG divergence (recall section 3c). However, as noted above, Simmons and Hoskins (1976) find remarkable agreement between PE and QG divergence in their simulations. The right column uses all the NLVE terms. The pattern of LC for the QG terms is similar to the full NLVE pattern. The most obvious difference is that the full system has much larger amplitude at the lowest levels (e.g., 900 mb). This difference is mainly due to the relative vorticity times divergence term, ZD. The similarity follows because the LC patterns at 200 and 500 mb are largely due to the rotational wind advection term RA, and the pattern at 900 mb largely reflects the term FD (Coriolis times divergence). While RA dominates the solution above low levels, the differences between RA and LC are important for understanding shape and growth changes. One obtains a crude estimate of growth changes by comparing the peak values of dipole couplets. The difference between the extrema in the couplet about the positive ζ maximum is about 5.4 in the QG solution and 7.3 in the full solution at 500 mb. At 200 mb the difference is also greater for the full solution. At 900 mb the full solution is much larger. The QG system appears to underestimate the growth at all levels, especially low levels. The difference between the extrema in the couplet northeast of the low at high levels (e.g., 200 mb) appears to favor more ridging in the full solution. These changes to growth may be the

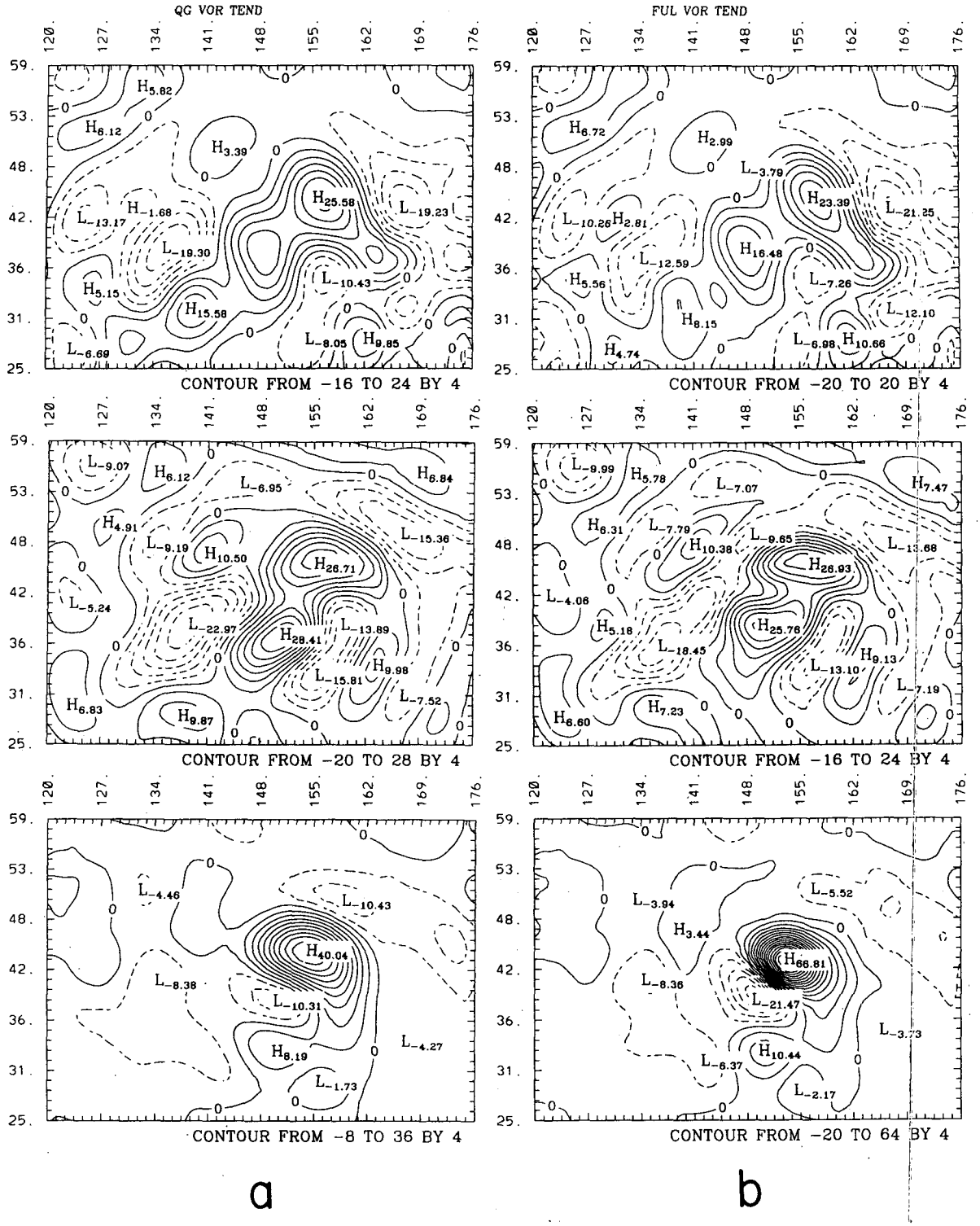

FIG. 7. Two estimates of the local change of relative vorticity (LC) by summing terms on the right-hand side of Eq. (1), the NLVE. The left column includes "quasigeostrophic" terms: RA, FD, and CR, where total wind divergence, not QG system divergence, is used in term FD. The right column includes all the terms.

most easily seen effect of including the non-QG terms, but there are also changes to the structure. For example, the separation between the extrema in the couplet about the upper ζ maximum (e.g., at 500- and 200-mb levels) is slightly larger and oriented with a slightly greater poleward component. This pattern could imply a faster motion of the trough, including a more poleward direction, or may indicate a broadening of the trough.

The results in Fig. 7 may be compared with some prior work using actual models. Lystad (1977) compares the forecasts made by QG and nonlinear BE models. Lystad reports that the BE model "may develop deeper cyclones" in rough agreement with the discussion in the preceding paragraph. Lystad also reports that BE model simulations are not as smooth as for the QG model and comments that the non-QG terms "have a smaller scale than the other terms." In another modeling study, Daley (1982) verified forecasts made by the QG, linear BE, and nonlinear BE systems against a primitive equations (PE) solution. Daley does not discuss individual cyclones but he does plot zonal and vertical average errors decomposed by length scale. Daley finds the cyclone-scale and shorter waves to be much better treated in the BE model than the QG. Neither model did well with the longest waves. Daley reports that his results are consistent with the extensive discussion of intermediate models in Gent and McWilliams (1982). Simmons and Hoskins (1976) examine various properties of idealized cyclones developing in QG and PE versions of their (linear) normal-mode model. Simmons and Hoskins compare QG and PE solutions developing along jets; the PE solutions generally have slower phase speed and again have faster growth rate.

Another type of intermediate model is the semigeostrophic (SG) system (e.g., Hoskins and West 1979). Snyder et al. (1991) compare SG and PE simulations of baroclinic development on a jet having uniform potential vorticity. Even though the SG solutions (by means of the coordinate transform) create asymmetry between the low and high, the PE solutions have even deeper lows and weaker highs. Unlike their QG or SG results, the PE solutions have northwest–southeast horizontal tilts, allow the trough axis to become more vertical, and have better frontal development. Snyder et al. attribute much of the difference to the lack of ageostrophic vorticity in the SG model.

We have considered why terms VA, ZD, and TT have traditionally been neglected in scale analysis. Several influential writings have argued that various combinations of these three terms are negligible. In contrast, some other past reports indicate that these terms might be individually or even collectively significant. We briefly discuss some scale analysis pitfalls as well as directly calculate various sums of these three terms. We find some cancellation among combinations of VA, ZD, and TT, but we also find a similar amount of reinforcement. Hence, summing these terms is not sufficient to make their contribution an order of magnitude less than FD.

It is beyond the scope of this article to judge the impact of the higher-order terms in theoretical models because a term's amplitude, areal extent, and interaction with other terms must be considered. However, it may be useful to propose a rough, qualitative grouping of the terms. Our grouping would be as follows. The first and largest group includes RA (mainly propagation) and FD. The second group includes TT, ZD, and DA. While we report sizes in the second group that are comparable to the first group, we have ranked these terms lower because they depend more strongly on the amplitude of the cyclone and because their areal extent is smaller. The third group includes CR and VA. Each term in a group is approximately *one-half* to *one-third* the size of a term in the preceding group. Term CD would be an order of magnitude smaller than the third group.

If one were designing a model, one would prefer to use these terms in combinations. For example, one would not include TT without including VA. A similar recommendation can be made for DA, ZD, and FD (if the Coriolis parameter is allowed to vary). As pointed out by Arnason and Carstensen (1959), only including part of one of these combinations may create spurious sources or sinks of vorticity. A system that includes all the NLVE terms discussed here is the balance equations.

The divergence term is incorporated into QG models by means of the adiabatic equation. The nature of that expression for D varies with the model. Hence, a more advanced model has both direct changes (additional terms in the NLVE) as well as indirect changes (a better estimate of D). Two approximations to D were tested. The ϕ form, requiring fewer approximations, does a much better job of matching extrema found in the PE data.

Acknowledgments. The author performed this research while on sabbatical visit to NCAR. He is grateful for the financial and computing resources provided by the Climate and Global Dynamics Division, which sponsored his stay. He is thankful for a wide variety of assistance from the NCAR staff. Particular thanks are directed to J. Tribbia, G. Branstator, L. Buja, and J. Lee. He also acknowledges the many helpful comments from the anonymous reviewers.

REFERENCES

Arnason, G., and L. Carstensen, 1959: The effects of vertical vorticity advection and turning of the vortex tubes in hemispheric forecasts with a two-level model. *Mon. Wea. Rev.*, **87,** 119–127.

Bosart, L., and S. Lin, 1984: A diagnostic analysis of the Presidents' Day storm of February 1979. *Mon. Wea. Rev.*, **112,** 2148–2177.

Buja, L., 1994: CCM Modular Processor User's Guide. NCAR Tech. Note NCAR-TN-384+IA, 239 pp. [Available from NCAR CGD, P.O. Box 3000, Boulder, CO 80307.]

Carlson, T., 1991: *Mid-Latitude Weather Systems.* Harper Collins, 507 pp.

Charney, J., 1962: Integration of the primitive and balance equations. *Proc. Int. Symp. Numerical Weather Prediction,* Tokyo, Japan, Meteor. Soc. Japan, 131–152.

Daley, R., 1982: A non-iterative procedure for the time integration of the balance equations. *Mon. Wea. Rev.,* **110,** 1821–1830.

Dutton, J., 1986: *The Ceaseless Wind.* Dover, 617 pp.

Eady, E., 1949: Long waves and cyclone waves. *Tellus,* **1,** 33–52.

Gent, P., and J. McWilliams, 1982: Intermediate model solutions to the Lorenz equations: Strange attractors and other phenomena. *J. Atmos. Sci.,* **39,** 3–13.

Grotjahn, R., 1993: *Global Atmospheric Circulations, Observations and Theories.* Oxford University Press, 430 pp.

——, 1996: Composite trough evolution of selected west Pacific extratropical cyclones. *Mon. Wea. Rev.,* **124,** 1470–1479.

——, and C.-H. Wang, 1990: Topographic linear instability on a sphere for various ridge orientations and shapes. *J. Atmos. Sci.,* **47,** 2249–2261.

Holton, J., 1992: *An Introduction to Dynamic Meteorology.* 3d ed. Academic Press, 507 pp.

Hoskins, B. J., and N. V. West, 1979: Baroclinic waves and frontogenesis. Part II: Uniform potential vorticity jet flows—Cold and warm fronts. *J. Atmos. Sci.,* **36,** 1663–1680.

Krishnamurti, T., 1968: A study of a developing wave cyclone. *Mon. Wea. Rev.,* **96,** 208–217.

Lystad, M., 1977: A general balanced model for numerical weather prediction. *Beitr. Phys. Atmos.,* **50,** 41–54.

McWilliams, J., and P. Gent, 1980: Intermediate models of planetary circulations in the atmosphere and ocean. *J. Atmos. Sci.,* **37,** 1657–1678.

Palmén, E., and C. Newton, 1969: *Atmospheric Circulations Systems, Their Structure and Physical Interpretation.* Academic Press, 603 pp.

Petterssen, S., 1956: *Weather Analysis and Forecasting.* Vol. 1, *Motion and Motion Systems,* McGraw-Hill, 428 pp.

Reed, R., and F. Sanders, 1953: An investigation of the development of a mid-tropospheric frontal zone and its associated vorticity field. *J. Meteor.,* **10,** 338–349.

Simmons, A. J., and B. J. Hoskins, 1976: Baroclinic instability on the sphere: Normal modes of the primitive and quasi-geostrophic equations. *J. Atmos. Sci.,* **33,** 1454–1477.

Snyder, C., W. C. Skamarock, and R. Rotunno, 1991: A comparison of primitive-equation and semi-geostrophic simulations of baroclinic waves. *J. Atmos. Sci.,* **48,** 2179–2194.

Sutcliffe, R., 1947: A contribution to the problem of development. *Quart. J. Roy. Meteor. Soc.,* **73,** 370–383.

Whitaker, J., L. Uccellini, and K. Brill, 1988: A model-based diagnostic study of the rapid development phase of the Presidents' Day cyclone. *Mon. Wea. Rev.,* **116,** 2337–2365.